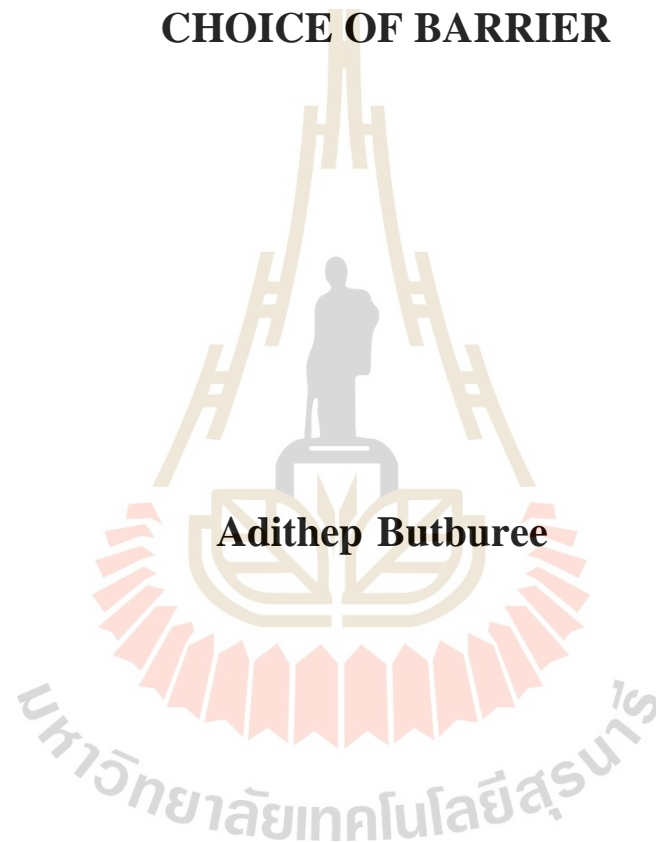


**THEORETICAL STUDY OF ELECTRICAL
TRANSPORT ACROSS FERROMAGNET-BARRIER-
FERROMAGNET TRILAYERS: EFFECT OF MATERIAL
CHOICE OF BARRIER**



**A Thesis Submitted in Partial Fulfillment of the Requirements for the
Degree of Master of Science in Applied Physics
Suranaree University of Technology
Academic Year 2018**

การศึกษาเชิงทฤษฎีของการขนส่งไฟฟ้าผ่านโครงสร้างสามชั้นเฟอร์โรแมกเนท-
ตัวกั้น-เฟอร์โรแมกเนท: ผลของการเลือกชนิดสารของตัวกั้น

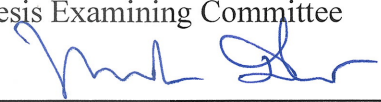


วิทยานิพนธ์นี้เป็นส่วนหนึ่งของการศึกษาตามหลักสูตรปริญญาวิทยาศาสตรมหาบัณฑิต
สาขาวิชาฟิสิกส์ประยุกต์
มหาวิทยาลัยเทคโนโลยีสุรนารี
ปีการศึกษา 2561

**THEORETICAL STUDY OF ELECTRICAL TRANSPORT ACROSS
FERROMAGNET-BARRIER-FERROMAGNET TRILAYERS:
EFFECT OF MATERIAL CHOICE OF BARRIER**

Suranaree University of Technology has approved this thesis submitted in partial fulfillment of the requirements for a Master's Degree.

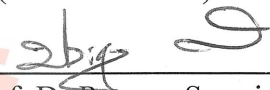
Thesis Examining Committee

x 
(Assoc. Prof. Dr. Panomsak Meemon)

Chairperson

x 
(Assoc. Prof. Dr. Puangratana Pairor)

Member (Thesis Advisor)


(Assoc. Prof. Dr. Prayoon Songsiriritthigul)

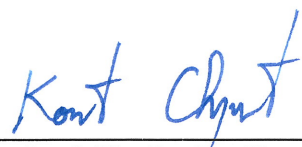
Member


(Assoc. Prof. Dr. Sirichok Jungthawan)

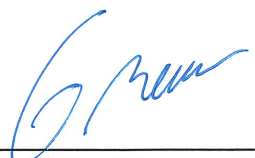
Member


(Asst. Prof. Dr. Michael F. Smith)

Member


(Assoc. Prof. Flt. Lt. Dr. Kontorn Chamniprasart)

Vice Rector for Academic Affairs
and Internationalization


(Assoc. Prof. Dr. Worawat Meevasana)

Dean of Institute of Science

อดิเทพ บุตรบุรี : การศึกษาเชิงทฤษฎีของการขนส่งไฟฟ้าผ่านโครงสร้างสามชั้นเฟอร์โรแมกเนต-ตัวกั้น-เฟอร์โรแมกเนต : ผลของการเลือกชนิดสารของตัวกั้น (TRANSPORT ACROSS FERROMAGNET-BARRIER-FERROMAGNET TRILAYERS : EFFECT OF MATERIAL CHOICE OF BARRIER). อาจารย์ที่ปรึกษา : รองศาสตราจารย์ ดร.พวงรัตน์ ไพเราะ, 46 หน้า.

ความต้านทานไฟฟ้า/ เฟอร์โรแมกเนติกแบบสามชั้น

วิทยานิพนธ์มหาบัณฑิตฉบับนี้เป็นงานวิจัยเชิงทฤษฎีศึกษาเกี่ยวกับความต้านทานไฟฟ้าในรอยต่อสามประเภทได้แก่ โลหะแม่เหล็กประเภทเฟอร์โรแมกเนติก/ฉนวน/โลหะแม่เหล็กประเภทเฟอร์โรแมกเนติก โลหะแม่เหล็กประเภทเฟอร์โรแมกเนติก/โลหะที่ไม่เป็นแม่เหล็ก/โลหะแม่เหล็กประเภทเฟอร์โรแมกเนติก และโลหะแม่เหล็กประเภทเฟอร์โรแมกเนติก/โลหะแม่เหล็กประเภทเฟอร์โรแมกเนติก/โลหะแม่เหล็กประเภทเฟอร์โรแมกเนติก โดยการประยุกต์ตามแบบจำลองทางทฤษฎีของชลอนิวสกี และรวมถึงผลของค่าสนามแม่เหล็กขนาดเล็ก ใช้การคำนวณทางทฤษฎีเพื่อพิจารณาผลกระทบของชั้นกั้นกลางที่เป็นฉนวนสำหรับรอยต่อประเภทแรกและดูประสิทธิภาพของค่าต้านทานไฟฟ้าในสองรอยต่อสุดท้าย และความหนาของชั้นกลางในทุกกรณี พบว่า ในรอยต่อที่ชั้นกั้นกลางเป็นฉนวน ค่าความต้านทานจะเพิ่มขึ้นตามความหนาของชั้นกั้นกลางนอกจากนี้ จะเห็นได้ว่าผลของพลังงานศักย์ชั้นกั้นกลางจะให้ค่าความต้านทานสูงสุดที่เฉพาะค่าเดียวและค่าสนามแม่เหล็กที่ทำให้ค่าความต้านทานสูงสุดแปรผันเป็นเส้นตรงกับต่างพลังงานศักย์ชั้นกั้นกลาง ในรอยต่อที่ชั้นกั้นกลางสองชนิดสุดท้ายได้แสดงให้เห็นถึงผลของค่าความต้านทานของแต่ละความหนาที่ขึ้นกับผลของความสูงกำแพงศักย์บริเวณรอยต่อค่าที่ได้แสดงให้เห็นถึงผลกระทบดังกล่าวมีความสำคัญต่อค่าความต้านทานเช่นกัน

สาขาวิชาฟิสิกส์

ปีการศึกษา 2561

ลายมือชื่อนักศึกษา

อดิเทพ บุตรบุรี

ลายมือชื่ออาจารย์ที่ปรึกษา

รองศาสตราจารย์ ดร.พวงรัตน์ ไพเราะ

ADITHEP BUTBUREE : THEORETICAL STUDY OF ELECTRICAL
TRANSPORT ACROSS FERROMAGNET-BARRIER-FERROMAGNET
TRILAYERS : EFFECT OF MATERIAL CHOICE OF BARRIER. THESIS
ADVISOR : PUANGRATANA PAIROR, Ph.D. 46 PP.

MAGNETORESISTANCE/ FERROMAGNETIC TRI-LAYER

This master thesis is a theoretical study of the magnetoresistance of three types of heterostructures: ferromagnetic metal/insulator/ferromagnetic metal, ferromagnetic metal/nonmagnetic metal/ferromagnetic metal and ferromagnetic metal/ferromagnetic metal/ferromagnetic metal junctions. By modifying the theoretical model used by Slonczewski with the inclusion of a small applied magnetic field, we theoretically consider the impact of the insulating barrier potential for the first type of junction, the quality of the two contacts for the last two types of junctions, and the thickness of the layer in all cases. We find that higher insulating barrier potential and thicker barrier can each boost the magnetoresistance. The magnetoresistance is increased with the applied magnetic field in all cases and reaches its maximum value at a particular magnetic field strength that depends on the thickness of layer. In the last two types of junctions the Delta-function potential barriers can have a large effect on the magnetoresistance.

School of Physics

Academic Year 2018

Student's Signature Adithes Butburee

Advisor's Signature Puangratana Pairor

ACKNOWLEDGEMENTS

My thesis could not be completed without help and support from many people. First of all, I would like to thank my advisor Assoc. Prof. Dr. Puangratana Pairor for giving me a chance to learn about condensed matter physics. I deeply appreciate her guidance, teaching, encouragement, support, patience and valuable advice. I also would like to thank other thesis committee members Asst. Prof. Dr. Panomsak Meemon, Assoc. Prof. Dr. Prayoon Songsiriritthigul, Assoc. Prof. Dr. Sirichok Jungthawanand and Asst. Prof. Dr. Michael F. Smith, for their valuable time and advice on research aspects for my thesis.

I am also thankful to Miss Natthagrittha Nakhonthong, who has helped me throughout the getting-master-degree process, from technical assistance on mathematica to kind encouragements.

Lastly, I would like to give big thank to everyone in condensed matter physics group and nuclear and particle group, my family, all my teachers, and my girlfriend for supporting me to everything I needed and every time when I have some problems.

Adithep Butburee

CONTENTS

	Page
ABSTRACT IN THAI.....	I
ABSTRACT IN ENGLISH	II
ACKNOWLEDGEMENTS.....	III
CONTENTS.....	IV
LIST OF FIGURES	VI
CHAPTER	
I INTRODUCTION	1
1.1 Literature review.....	2
1.2 Scope and outline of thesis	9
II METHOD OF CALCULATION.....	11
2.1 The slonczewski model.....	12
2.2 Modification of Slonczewski's model.....	16
2.3 Conductivity from transmission probability.....	18
III MAGNETORESISTANCE RESULTS AND DISSCUSSION.....	20
3.1 Magnetoresistance of FM/insulator/FM systems.....	20
3.2 Magnetoresistance of FM/non-magnetic metal/FM systems.....	25
3.3 Magnetoresistance of FM/FM/FM systems.....	29
IV CONCLUSION	33
REFERENCES	34

CONTENT (Continued)

	Page
CURRICULUM VITAE.....	46



LIST OF FIGURES

Figure	Page
1.1 Spin polarization of the tunneling conductance as a function of the normalized potential barrier height for various values of $k_{\uparrow}/k_{\downarrow}$, taken from Slonczewski.....	7
1.2 Angular dependence of the resistance of a CoFe/Al ₂ O ₃ /Co junction measured in an external magnetic field lower than the exchange energy of one electrode but higher than the exchange energy of the other electrode.....	8
1.3 Diagram of the geometry of ferromagnet-barrier-ferromagnet junctions.	9
2.1 Schematic potential energy for two metallic ferromagnets, separated by an insulating barrier of thickness L	12
2.2 The sketches of excitation energy spectra of FM/Insulator/FM junctions.....	14
3.1 Magnetoresistance as a function of magnetic field with thickness of the insulating layer $L = 6/k_F$ and $U_0 = 0.4\varepsilon_F$	21
3.2 (a) Magnetoresistance as a function of magnetic field with varying thickness L of the insulating layer and $U_0 = 0.4\varepsilon_F$	22
3.3 Magnetoresistance as a function of magnetic field with thickness $L = 6/k_F$ of the insulating layer when $U_0 = 0.33\varepsilon_F$ and $U_0 = 0.35\varepsilon_F$	23
3.4 The critical magnetic field CB_c/ε_F versus potential barrier U_0/ε_F	24
3.5 (a) graph magnetoresistance versus thickness when potential barrier $U_0 = 0.4\varepsilon_F$ our work.....	25

LIST OF FIGURES (Continued)

Figure	Page
3.6 Magnetoreistance vs B at different values of L.....	26
3.7 The graph shows MR vs CB/ε_F (a).....	27
3.8 The graph shows MR vs thickness of middle layer (a)	28
3.9 Shows the variation of magnetoresistance (MR) values with external magnetic fields (CB) which chance $\varepsilon_{F2}/\varepsilon_{F1}$ equal to 0.9 to 1.1	29
3.10 Magnetoreistance vs B at different values of L. $Z_1 = Z_2 = 1$ and $\varepsilon_{F2}/\varepsilon_{F1} = 1$	30
3.11 Represents the change of value magnetoresistance vs thickness L at various values of the parameter $Z = 0, 0.5, 0.7$	31
3.12 Represents the change of value magnetoresistance vs thickness L at various values of the parameter $Z = 0, 0.5, 0.7$	31
3.13 Show the result of magnetoresistance in a function of external magnetic field (CB/ε_F) of $Z_1 = Z_2$, (a) and $Z_1 \neq Z_2$ (b).	32

CHAPTER I

INTRODUCTION

Spintronics research field was born in 1988, when two research groups, one led by Gruenberg (Gruenberg et al., 1989) and the other by Fert (Fert et al., 1988), discovered giant magnetoresistance effect in the alternating layer structures of ferromagnetic metals and non-magnetic metals. The discovery was made possible with the molecular beam epitaxy technique, which enabled them to control the thickness of each non-magnetic layer to be of order 1 – 2 nm. This range of thickness was key to obtaining the antiparallel direction of the magnetizations in the neighboring ferromagnetic layers. They found the resistances of the magnetic multilayers can change dramatically with an applied magnetic field. That is, when their magnetizations are antiparallel in the absence of an applied field, the resistance of the system is high, but in the presence of the field they are in parallel and the resistance is lower. Specifically, Gruenberg's group found that the resistance of a trilayer Fe/Cr/Fe system was decreased by 3% at room temperature and by 10% at 5 K (Gruenberg et al., 1989). In the case of $(\text{Fe/Cr})_n$, where n is as high as 60, Fert's group et al. reported a maximum resistance decrease of 50% at 4.2 K (Gruenberg et al., 1989). The ability to control the “giant” change in resistance with small magnetic field led to the applications in sensors and magnetic random access memories, which are capable of quick readout for magnetic disks.

1.1 Literature review

Historically the change of resistance of a ferromagnetic metal in an applied field, or magnetoresistance, was first discovered in Ni and Fe by Lord Kelvin in 1856 (Thomson et al., 1857). He measured the change of resistance to be no more than 5% at room temperature in an external field. In 1975, Jullière was first to observe the tunneling magnetoresistance effect in a junction consisting of two ferromagnetic electrodes, Fe and Co, isolated by a Ge film of 10–15 nm thick. He controlled the directions of the magnetizations of the two electrodes by varying the strength of applied magnetic field. When the field is stronger than the exchange energies of both electrodes, the magnetizations were in parallel. When the field strength is in between the two exchange energies, the magnetizations were in antiparallel. He measured the change in the conductance G of the junction in a zero field relative to that in the magnetic field \vec{B} , or the tunneling magnetoresistance ratio

$$MR \equiv \frac{G(\vec{B} \neq 0) - G(\vec{B} = 0)}{G(\vec{B} = 0)} \quad (1.1)$$

and found its maximum of 14% at 4.2 K (Jullière et al., 1975). Although the effect roused research interest for both the underlying mechanism and potential applications, due to the difficulties in fabrication process to achieve reproducible and robust tunnel junctions the magnetic tunneling junctions were not widely experimentally studied after Jullière's publication until the late 1980s. As soon as more reliable experimental techniques that can precisely control the thickness of the insulating layers like molecular beam epitaxy and later ultrahigh vacuum dc magnetron sputtering were realized, the research interest in magnetoresistance was renewed. As mentioned earlier, the thickness in nanoscale of the non-magnetic layers in-between the alternating

ferromagnetic layers controls the relative directions of the magnetizations of the ferromagnetic layers. Appropriate thickness of the non-magnetic layers causes the magnetizations of the two adjacent ferromagnetic layers to have opposite direction (Ruderman et al., 1954; Kei et al., 1957; Kasuya et al., 1954). When non-magnetic layers are metallic like in the case of Fert's and Gruenberg's work, the highest magnetoresistance is around add 10-50% (Fert et al., 1988). Once research groups were able to make multilayer magnetic junctions with the non-magnetic layers being insulators, the systems with higher value of magnetoresistance were discovered. Al_2O_3 and MgO are examples of popular insulating oxide layers that have been incorporated into tunneling magnetic junction structures.

In 1995, Moodera (Moodera et al., 1995) and his colleagues found the magnetoresistance of 24% at 4.2 K and 12% at room temperature in $\text{CoFe}/\text{Al}_2\text{O}_3/\text{Co}$ systems, and Miyazaki (Miyazaki et al., 2010) found a resistance decrease of 30% at 4.2 K and 18% at room temperature of $\text{Fe}/\text{Al}_2\text{O}_3/\text{Fe}$ junction. A few years later, P. K. Wong (Wong et al., 1998) reported that their $\text{Nb}/\text{Fe}/\text{Al}_2\text{O}_3\text{-Al}/\text{CoFe}/\text{Nb}$ multilayer junctions had the tunneling magnetoresistance of 6.2% at room temperature and 9.2% at 77 K. In 2002, S. Yuasa and his group (Yuasa et al., 2002) had combined molecular beam epitaxy technique and the subsequent microfabrication processes to precisely control the thickness of each layer in the structure $\text{NiFe}/\text{Al}_2\text{O}_3/\text{Cu}/\text{Co}$. They focused their study on how the tunneling magnetoresistance changes with the thickness of the Cu layer. They found that the effect of the thickness of the Cu is interpreted in terms of the formation of spin-polarized resonant tunneling. The amplitude of the oscillation is so large that even the sign of the tunnel magnetoresistance alternates. In 2003, (Hyung Yu et al., 2003) were able to achieve the tunneling magnetoresistance of 45.5% for the

structure NiFe/Al-oxide/CoFe/IrMn/NiFe/Ta at room temperature. Many other research groups had also produced tunneling magnetic junctions with Al-oxide and the insulating layer and achieved tunneling magnetoresistance measurements of 50% at room temperature (Okamura et al., 2005; Bai et al., 2008; Barraud et al., 2010; Joo et al., 2014; shvets et al., 2005).

In addition to Al-oxide, MgO is also incorporated into tunneling magnetic junction as the insulating layer. In 2003, J. Faure-Vincent (Faure-Vincent et al., 2003) used the molecular beam epitaxy technique to make Fe/MgO/Fe junctions and reported their tunneling magnetoresistance as high as 100% at 80K and 67% at room temperature. This value was high than that of the junction with Al-oxide layer and sparked more work on the junctions with MgO as the insulating layer and reached the tunneling magnetoresistance as high as 138% at 80 K (Philip et al., 2009; Hatanaka et al., 2015; Almasi et al., 2017; Ikeda et al., 2010; Yuasa et al., 2004; Tao et al., 2014; García-García et al., 2011; Bai et al., 2012; Liang et al., 2014; Tsunegi et al., 2009; García-García et al., 2010; Yang et al., 2010). These experimental works implied that the material used as the insulating layer affects very much the tunneling magnetoresistance.

There are many approaches one can use to understand the tunneling magnetoresistance. Here, we focus on two approaches: Jullière's and Slonczewski's.

In 1975, Jullière, who did the first experiment on the tunneling magnetoresistance, was also the first to use a simple theoretical model to describe it. He used Bardeen's description of tunneling across an insulating barrier. In Bardeen's approach, which was based on the standard time-dependent perturbation theory, the

tunneling current density is equal to the net rate of transfer of electrons between the electrodes (Bardeen et al., 1961):

$$J = \frac{2\pi e}{\hbar} \sum_{ij} |b_{ij}|^2 [f(\varepsilon_i - \mu_L) - f(\varepsilon_j - \mu_R)] \delta(\varepsilon_i - \varepsilon_j), \quad (1.2)$$

where i, j respectively labels the electron states of the left and right electrodes, b_{ij} is the tunneling matrix element between these states, $f(\varepsilon - \mu)$ is the Fermi-Dirac distribution function, and μ is the associated chemical potential. Using Bardeen's expression for the current and two assumptions: the electron spin is conserved and b_{ij} are the same for all states, Jullière obtained the conductances, G_P and G_{AP} , for the parallel and antiparallel magnetizations of the two electrodes at zero temperature respectively as follows:

$$G_P = \frac{1}{R_P} = \frac{e^2}{\hbar} |b|^2 [D_L^\uparrow(\varepsilon_F) D_R^\uparrow(\varepsilon_F) + D_L^\downarrow(\varepsilon_F) D_R^\downarrow(\varepsilon_F)] \quad (1.3)$$

$$G_{AP} = \frac{1}{R_{AP}} = \frac{e^2}{\hbar} |b|^2 [D_L^\uparrow(\varepsilon_F) D_R^\downarrow(\varepsilon_F) + D_L^\downarrow(\varepsilon_F) D_R^\uparrow(\varepsilon_F)] \quad (1.4)$$

where $D_i^s(\varepsilon_F)$ is the density of states of electrode i for spin s and R_P, R_{AP} are the corresponding resistance. Jullière tunneling magnetoresistance ratio is defined as

$$\text{TMR} \equiv \frac{G_P - G_{AP}}{G_{AP}} = \frac{R_{AP} - R_P}{R_P} \quad (1.5)$$

In term of spin polarization, $P \equiv \frac{D^\uparrow - D^\downarrow}{D^\uparrow + D^\downarrow}$,

$$\text{TMR} = \frac{2P_L P_R}{1 - P_L P_R}. \quad (1.6)$$

This formula gave a value of 26% for Fe/Ge/Co junctions, which is higher than the maximum measured value of 14%. The discrepancy may be due to the spin-flip scattering and the magnetic coupling between the two electrodes (Jullière et al., 1975).

In 1989, Slonczewski (Slonczewski et al., 1989) approximated the electron energy dispersion relation of two ferromagnetic metals as two parabolic bands shifted rigidly by the exchange splitting of the spin bands. He solved the Schrödinger equation of two identical ferromagnetic films separated by a rectangular potential barrier, and obtained the conductance G as a function of the relative magnetization direction of the two films, specified by an angle θ .

$$G(\theta) = G_0(1 + P^2 \cos \theta), \quad (1.7)$$

where P is the effective spin polarization of tunneling electrons:

$$P = \left(\frac{k^\uparrow - k^\downarrow}{k^\uparrow + k^\downarrow} \right) \left(\frac{\kappa^2 - k^\uparrow k^\downarrow}{\kappa^2 + k^\uparrow k^\downarrow} \right), \quad (1.8)$$

where $\kappa = \sqrt{2mU/\hbar^2}$, m is the electron effective mass, U is the barrier potential, ε_F is the Fermi energy of each ferromagnetic metal, and $k_\uparrow, k_\downarrow = \sqrt{(2m/\hbar^2)(\varepsilon_F \mp h)}$ are the Fermi wave vectors of the bands for spin-up and spin-down electrons respectively.

In the $U \gg \varepsilon_F$ limit, Slonczewski's model provides the same results as Jullière's model. When U is not large, the spin polarization is decreased with decreasing U and flips its sign for small enough barrier potential (Figure 1.1). This result was the first to indicate that the spin polarization of the tri-layered system can be affected significantly by the physical properties of the middle layer.

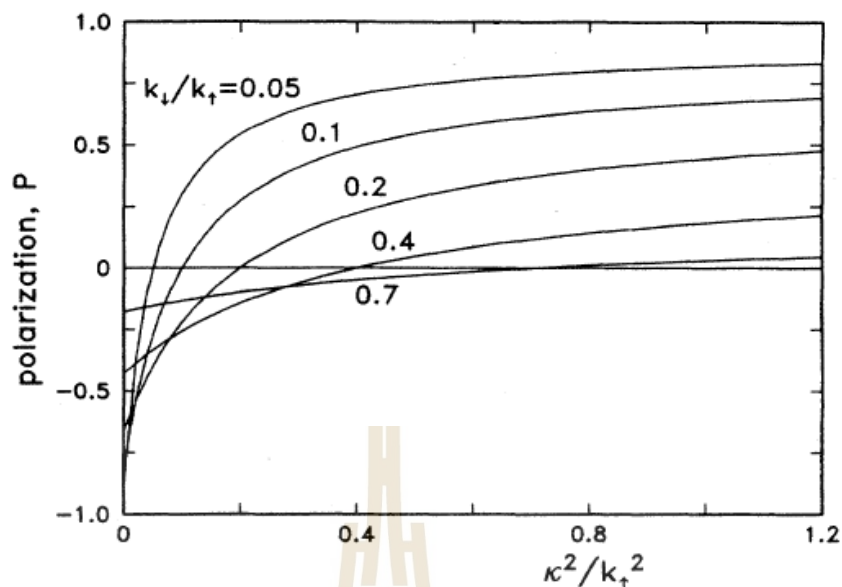


Figure 1.1 Spin polarization of the tunneling conductance as a function of the normalized potential barrier height for various values of k_t/k_l , taken from Slonczewski (Slonczewski et al., 1989).

The cosine dependence of the conductance, predicted by Slonczewski's model, was experimentally confirmed by Moodera and Kinder (Moodera et al., 1995; Kinder et al., 1995). They performed a tunneling experiment on a tri-layered system containing different ferromagnetic films in an external field stronger than the coercive field of one electrode but lower than that of the other. This condition made the magnetization of the harder electrode point in a particular direction during the experiment and made it possible to control the direction of the magnetization of the softer electrode by the external field. Their resistance measurements showed dependence on the field direction with respect to the magnetization of the harder electrode as $\cos \theta$ (Figure 1.2).

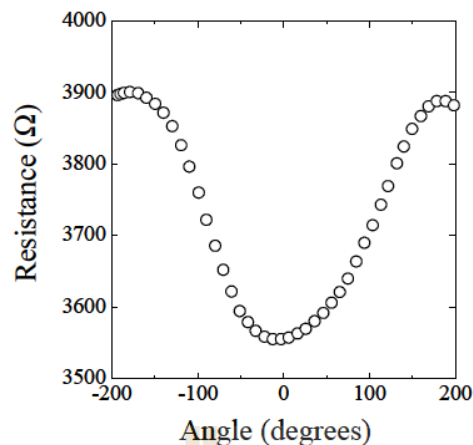


Figure 1.2 Angular dependence (θ) of the resistance of a CoFe/Al₂O₃/Co junction measured in an external magnetic field lower than the exchange energy of one electrode but higher than the exchange energy of the other electrode (Moodera et al., 1995; Kinder et al., 1995).

In 1998, Yunong Qi, D. Y. Xing, and Jinming Dong showed that the results from the Slonczewski's model with the delta-function as the barrier potential and those from the Julliere formula have the same form in the tunneling limit. They confirmed the results, which were also obtained by Slonczewski, that tunneling magnetoresistance ratio is sensitive to the angle between the magnetization of the two adjacent ferromagnetic layers and their exchange energies. Also, the magnetoresistance ratio is insensitive to the height and width of the potential barrier in the tunneling limit. Their results indicated that Slonczewski's theoretical model can be used to study wider variety of junction types than Julliere's model (Julliere et al., 1998). In all these approaches the researchers did not directly put the applied magnetic field in their calculations. The effect of the applied field magnetic field was indirectly included through the difference in densities of states of the spin-up and spin-down electrons (in

Julliere's case) or the change in the direction of magnetization of one of the ferromagnetic layers (Slonczewski's case).

1.2 Scope and outline of thesis

The system that is studied in this thesis is a ferromagnet-barrier-ferromagnet structure (as shown in Figure 1.3). We theoretically investigate the effect of material choice of the middle layer between two the ferromagnetic metals on the electrical transport under external magnetic field. We will assume purely ballistic scattering and use a one-electron model in one dimension to describe the trilayer structure. The three choices of materials are an insulator, a non-magnetic metal, and a ferromagnetic metal. The conductivity, which is the inverse of resistivity, of the trilayers at zero temperature is obtained from the transmission probabilities in a small applied magnetic field. We use Slonczewski's model to investigate the tunneling magnetoresistance by directly incorporating the magnetic field into the model.

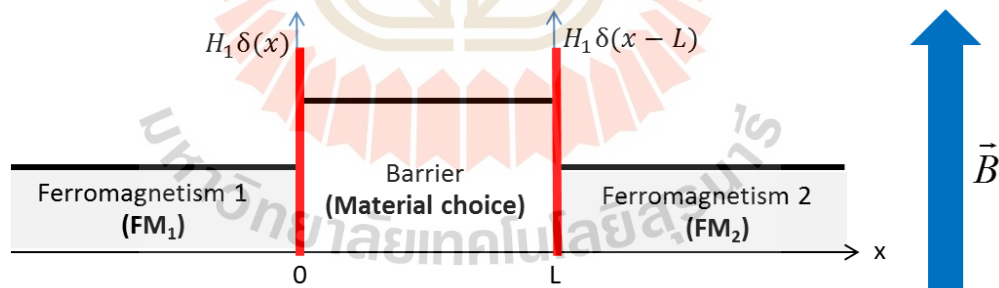


Figure 1.3 Diagram of the geometry of ferromagnet-barrier-ferromagnet junctions. Both ferromagnet occupy the spaces where $x < 0$, $x > L$ and the material choice occupies the space where $0 < x < L$. The two insulating layers at $x = 0$ and $x = L$, which are represented by delta-function barrier potentials of height H_1 and H_2 , L is the thickness of material choice.

In the next chapter, we present the details of the method we use to calculate the magnetoresistance of each junction. We present the results from the calculations in Chapter III. We provide a summary and discussion of main results in Chapter IV.



CHAPTER II

METHOD OF CALCULATION

In this chapter, we will describe the method of calculation used in our work to calculate the magnetoresistance of our junctions of interest. We adapted Slonczewski's model to do so for our systems. In 1989, he theoretically analyzed the transmission of charge and spin currents through a rectangular barrier separating two free-electron like ferromagnetic metals (FM). He assumed arbitrary magnetization alignments of two ferromagnetic layers isolated by a non-magnetic insulating barrier. His model predicts dependence of the magnetoresistance on the angle between the two magnetizations and influence of tunneling barrier height on magnetic coupling between the two metals, thereby affecting the tunneling magnetoresistance in FM/insulator/FM junctions (Slonczewski et al., 1989).

In the next section, we will present his one-electron Hamiltonian and how he used the quantum scattering calculation to get transmission probability. Later on, we will explain how we modified the Hamiltonian to represent our tri-layered systems, in which the middle layer is non-magnetic metallic or ferromagnetic metal. We will also show how we obtained the magnetoresistance ratio from the transmission probability at the end of the chapter.

2.1 The Slonczewski model

In Slonczewski's model, the system is divided into 3 regions as depicted in Figure 2.1, region 1 ($x < 0$) and region 3 ($x > L$) are ferromagnetic metals with the molecular fields of \vec{h}_A and \vec{h}_B , respectively. The magnitudes of both fields are related to the ferromagnetic exchange couplings in both regions. He took both molecular fields to have the same magnitude: $|h_A| = |h_B| = h_0$, and set an angle of arbitrary θ to define the direction between \vec{h}_A and \vec{h}_B as shown in Figure 2.1. The middle layer or region 2 ($0 < x < L$) separates the two ferromagnetic metals. In his calculation, this layer is taken to be a non-magnetic insulator giving rise to a tunneling effect.

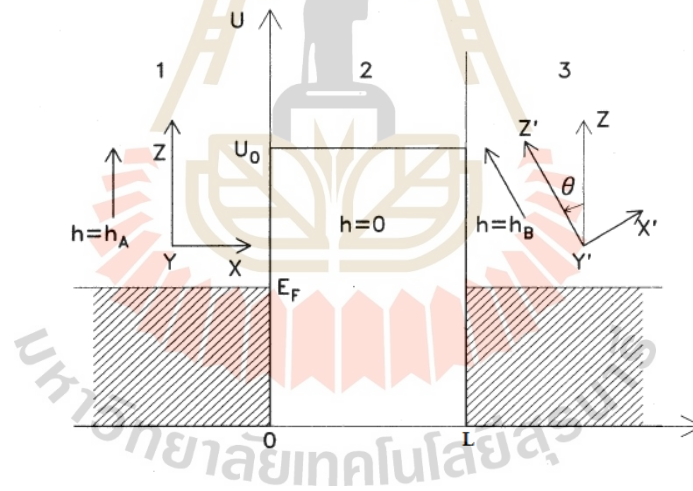


Figure 2.1 Schematic potential energy for two metallic ferromagnets, separated by an insulating barrier of thickness L . The molecular fields \vec{h}_A and \vec{h}_B form an angle of θ (Slonczewski et al., 1989).

The effective one-electron Hamiltonian takes the form:

$$\hat{H} = -\frac{\hbar^2}{2m} \frac{d^2}{dx^2} + U_0[\Theta(x) - \Theta(x - L)] - h_0\{\hat{z}\Theta(-x) + [\hat{z} \cos \theta - \hat{x} \sin \theta]\Theta(x - L)\} \cdot \vec{\sigma} - \varepsilon_F[\Theta(-x) + \Theta(x - L)], \quad (2.1)$$

where $\vec{\sigma}$ is the Pauli spin operator: $\vec{\sigma} = (\sigma_x, \sigma_y, \sigma_z)$ and

$$\sigma_x \equiv \begin{pmatrix} 0 & 1 \\ 1 & 0 \end{pmatrix} \quad \sigma_y \equiv \begin{pmatrix} 0 & -i \\ i & 0 \end{pmatrix} \quad \sigma_z \equiv \begin{pmatrix} 1 & 0 \\ 0 & -1 \end{pmatrix}.$$

Also, $\Theta(x)$ is the Heaviside step function.

Solving the time-independent Schrödinger equation, we obtain the eigenenergies of the electrons in region 1 and 3 as

$$E_1 = E_3 = \frac{\hbar^2 k_{1 \text{ or } 3}^2}{2m} \mp h_0 - \varepsilon_F, \quad (2.2)$$

where the minus and plus signs are for spin-up and spin-down electrons, respectively. k is the electron wave vector. The electron eigenenergies in the insulating layer (region 2) is,

$$E_2 = \frac{\hbar^2 K^2}{2m} + U_0. \quad (2.3)$$

K is the electron wave vector in this region. U_0 is the barrier potential energy, which is equal to half of the energy band gap of the insulating layer.

We consider only a ballistic scattering process; that is, we take $E_1 = E_2 = E_3 = E < U_0$. Consequently, k is real and $K \equiv i\kappa$ is imaginary. Figure 2.2 is the sketch of the energy spectra in three regions.

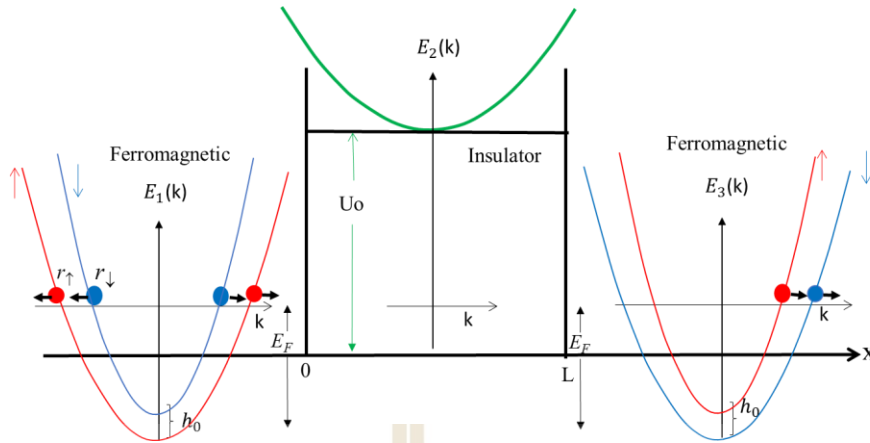


Figure 2.2 The sketches of excitation energy spectra of FM/Insulator/FM junctions. The arrows depict the directions of the electron spins.

In the scattering method, the electron wave function in each region can be written as follows.

In region 1 ($x < 0$) the wave function is a linear combination of one incident and two reflected waves. Because there are two possibilities of the spins for the incident electrons, in the case of spin-up incident electron, we have

$$\psi_{1\uparrow} = \begin{bmatrix} 1 \\ 0 \end{bmatrix} e^{ik_{1\uparrow}x} + r_{\uparrow} \begin{bmatrix} 1 \\ 0 \end{bmatrix} e^{-ik_{1\uparrow}x} + r_{\downarrow} \begin{bmatrix} 0 \\ 1 \end{bmatrix} e^{-ik_{1\downarrow}x}. \quad (2.4)$$

In the case of spin-down incident electron, we have

$$\psi_{1\downarrow} = \begin{bmatrix} 0 \\ 1 \end{bmatrix} e^{ik_{1\downarrow}x} + r_{\uparrow} \begin{bmatrix} 1 \\ 0 \end{bmatrix} e^{-ik_{1\uparrow}x} + r_{\downarrow} \begin{bmatrix} 0 \\ 1 \end{bmatrix} e^{-ik_{1\downarrow}x}. \quad (2.5)$$

r_{σ} are the reflection coefficients of the reflected electron waves with spin σ .

In region 2 ($0 \leq x \leq L$) the wave function takes the form

$$\psi_2 = \begin{bmatrix} c_{\uparrow} \\ c_{\downarrow} \end{bmatrix} e^{-\kappa x} + \begin{bmatrix} d_{\uparrow} \\ d_{\downarrow} \end{bmatrix} e^{\kappa x} \quad (2.6)$$

c_σ and d_σ are the decaying and growing exponential electron waves with spin σ in this region.

In region 3 ($x > L$) the wave function is the linear combination of two outgoing wave functions:

$$\psi_3 = t_\uparrow \begin{bmatrix} \cos \frac{\theta}{2} \\ \sin \frac{\theta}{2} \end{bmatrix} e^{ik_{3\uparrow}x} + t_\downarrow \begin{bmatrix} \sin \frac{\theta}{2} \\ -\cos \frac{\theta}{2} \end{bmatrix} e^{ik_{3\downarrow}x}. \quad (2.7)$$

t_σ are the transmission coefficients of the outgoing electron waves with spin σ . Is the angle between the majority spins of the FM in the region 3 and those of the FM in region 1.

These eight unknowns r_σ , c_σ , d_σ , t_σ , are obtained by solving eight equations of matching conditions for the wave functions and their slopes at the boundaries ($x = 0$ and $x = L$) in the system. The equations are

$$\psi_1(x = 0) = \psi_2(x = 0) \quad (2.8)$$

$$\psi_2(x = L) = \psi_3(x = L) \quad (2.9)$$

$$\frac{d\psi_2(x=0)}{dx} = \frac{d\psi_1(x=0)}{dx} \quad (2.10)$$

$$\frac{d\psi_3(x=L)}{dx} = \frac{d\psi_2(x=L)}{dx}. \quad (2.11)$$

The main goal is to find the transmission coefficients because we want to obtain the total transmission probability $T(E, \theta)$, which is defined as

$$T(E, \theta) \equiv \frac{1}{2} \left[\frac{k_{3\uparrow}(E)|t_\uparrow(E, \theta)|^2 + k_{3\downarrow}(E)|t_\downarrow(E, \theta)|^2}{k_{1\uparrow}(E)} + \frac{k_{3\uparrow}(E)|t_\uparrow(E, \theta)|^2 + k_{3\downarrow}(E)|t_\downarrow(E, \theta)|^2}{k_{1\downarrow}(E)} \right] \quad (2.12)$$

The former and the latter terms refer to the transmission probability of an incident spin-up electron and that of an incident spin-down electron respectively.

2.2 Modification of Slonczewski's model

The tri-layered systems of our interest are FM/insulator/FM, FM/non-magnetic metal/FM, and FM/FM/FM junctions. We take the magnetizations of the two adjacent FMs to be in opposite directions, and we want to investigate these systems in small applied magnetic field. So, we rewrite the Hamiltonian of for each type of the tri-layered system under the external magnetic field in the z-direction, based on the Slonczewski model, as follows:

- 1) FM/insulator/FM junction

$$\hat{H}_I = -\frac{\hbar^2}{2m} \frac{d^2}{dx^2} - U_0[\Theta(x) - \Theta(x-L)] - h_0\{\hat{z}\Theta(-x) - \hat{z}\Theta(x-L)\} \cdot \vec{\sigma} - \varepsilon_F[\Theta(-x) + \Theta(x-L)] + CB\hat{z} \cdot \vec{\sigma}. \quad (2.13)$$

$B\hat{z}$ is the external field pointing in the z direction and C is an appropriate constant.

- 2) FM/non-magnetic metal/FM junctions

$$\hat{H}_M = -\frac{\hbar^2}{2m} \frac{d^2}{dx^2} - h_0\{\hat{z}\Theta(-x) - \hat{z}\Theta(x-L)\} \cdot \vec{\sigma} - \varepsilon_{F2}[\Theta(x) - \Theta(x-L)] - \varepsilon_F[\Theta(-x) + \Theta(x-L)] + CB\hat{z} \cdot \vec{\sigma} + U_1\delta(x) + U_2\delta(x-L), \quad (2.14)$$

where ε_{F2} is the Fermi energy in region 2. $U_1\delta(x)$, $U_2\delta(x-L)$ represent the Dirac delta-function insulating barrier potential at the two interfaces.

- 3) FM/FM/FM junctions

$$\hat{H}_{FM} = -\frac{\hbar^2}{2m} \frac{d^2}{dx^2} - h_0\{\hat{z}\Theta(-x) - [\hat{z}\Theta(x) - \Theta(x-L)] + \hat{z}\Theta(x-L)\} \cdot \vec{\sigma} - \varepsilon_F\{\Theta(-x) + [\Theta(x) - \Theta(x-L)] + \Theta(x-L)\} + CB\hat{z} \cdot \vec{\sigma} + U_1\delta(x) + U_2\delta(x-L), \quad (2.15)$$

We take all the ferromagnetic layers to be the same material. Due to the fact that the related energy of the applied magnetic field used in the magnetoresistance

experiments (typically no more than a few Teslas) is so much smaller the Fermi energy of the ferromagnetic material that it only affects the spin parts, we approximate our eigenfunctions in all regions to be in the same propagating forms as in the case where there is no applied field.

Due to the RKKY interaction between the two ferromagnetic layers, their magnetizations are in opposite directions and we set θ in Equation (17) is $\pi/2$ to reflect this (Simon et al., 2005; Shuo Mi et al., 2011).

The wave function of electron in region 2 now takes the following form, for the case of FM/insulator/FM junctions:

$$\psi_2 = \begin{bmatrix} c_1 \\ 0 \end{bmatrix} e^{-k_{2\uparrow}x} + \begin{bmatrix} 0 \\ c_2 \end{bmatrix} e^{-k_{2\downarrow}x} + \begin{bmatrix} d_1 \\ 0 \end{bmatrix} e^{k_{2\uparrow}x} + \begin{bmatrix} 0 \\ d_2 \end{bmatrix} e^{k_{2\downarrow}x}. \quad (2.16)$$

$k_{2\uparrow}$ satisfies $E_2 = U_0 - \frac{\hbar^2 k_{2\uparrow}^2}{2m} + CB$ and $k_{2\downarrow}$ does $E_2 = U_0 - \frac{\hbar^2 k_{2\downarrow}^2}{2m} - CB$. Similarly, the electron wave function in region 2 of FM/non-magnetic metal/FM interfaces is

$$\psi_2 = \begin{bmatrix} c_1 \\ 0 \end{bmatrix} e^{ik_{2\uparrow}x} + \begin{bmatrix} 0 \\ c_2 \end{bmatrix} e^{ik_{2\downarrow}x} + \begin{bmatrix} d_1 \\ 0 \end{bmatrix} e^{-ik_{2\uparrow}x} + \begin{bmatrix} 0 \\ d_2 \end{bmatrix} e^{-ik_{2\downarrow}x} \quad (2.17)$$

where $k_{2\uparrow}$ satisfies $E_2 = \frac{\hbar^2 k_{2\uparrow}^2}{2m} - CB - \varepsilon_{F2}$ and $k_{2\downarrow}$ satisfies $E_2 = \frac{\hbar^2 k_{2\downarrow}^2}{2m} + CB - \varepsilon_{F2}$.

The electron wave function in region 2 of FM/FM/FM interfaces has the same form as

FM/non-magnetic metal/FM interfaces, where $k_{2\uparrow}$ now satisfies $E_2 = \frac{\hbar^2 k_{2\uparrow}^2}{2m} + h_2 -$

$CB - \varepsilon_{F2}$ and $k_{2\downarrow}$ does $E_2 = \frac{\hbar^2 k_{2\downarrow}^2}{2m} - h_2 + CB - \varepsilon_{F2}$.

We also add of the Dirac delta-function potential barriers at the two interfaces and the eight probability amplitudes $r_{\uparrow}, r_{\downarrow}, c_1, c_2, d_1, d_2, t_{\uparrow}, t_{\downarrow}$ can be obtained from slightly different matching conditions from before. These are

$$\psi_1(x = 0) = \psi_2(x = 0) \quad (2.18)$$

$$\psi_2(x = L) = \psi_3(x = L) \quad (2.19)$$

$$\frac{d\psi_2(x=0)}{dx} - \frac{d\psi_1(x=0)}{dx} = \frac{2mU_1}{\hbar^2} \psi(x = 0) \quad (2.20)$$

$$\frac{d\psi_3(x=0)}{dx} - \frac{d\psi_2(x=0)}{dx} = \frac{2mU_2}{\hbar^2} \psi(x = L). \quad (2.21)$$

The total transmission probability $T(E, \theta)$ still takes the same form as Eq. (2.15).

2.3 Conductivity from transmission probability

We will ultimately calculate the magnetoresistance MR from the conductivity, σ . That is,

$$\text{MR} = \frac{\sigma_P - \sigma_{AP}}{\sigma_{AP}} \quad (2.22)$$

where σ_P is the sum of the spin-up conductivity σ_{\uparrow} and spin-down conductivity σ_{\downarrow} when both ferromagnetic electrodes have parallel magnetizations, and σ_{AP} is the sum of σ_{\uparrow} and σ_{\downarrow} , when both ferromagnetic electrodes have antiparallel magnetizations. Below, we show how to obtain σ_{\uparrow} and σ_{\downarrow} from the transmission probability.

We can write the net current density of spin- s electrons across a junction, with an applied voltage $V = \mathbb{E}d$ across the junction of thickness d and with electric field \mathbb{E} , as

$$j_{net}^s = \sum_k e v_s T_s(k) [f(\varepsilon_k - eV) - f(\varepsilon_k)] \quad (2.23)$$

where e is the magnitude of an electron charge, $T_s(k)$ is the transmission probability of a spin- s electron, $f(\varepsilon_k)$ is the Fermi-Dirac distribution function, and \vec{v}_s is the velocity of the spin- s electron. Changing the summation in to an integral, one has for

one dimensional system,

$$j_{net}^s = \frac{Le}{2\pi} \int dk v_s T_s(k) [f(\varepsilon_k - eV) - f(\varepsilon_k)] \quad (2.24)$$

Because $v_s = \frac{1}{\hbar} \frac{d\varepsilon_k}{dk}$,

$$j_{net}^s = \frac{Le}{2\pi\hbar} \int_{-\infty}^{\infty} d\varepsilon_k T_s(\varepsilon_k) [f(\varepsilon_k - eV) - f(\varepsilon_k)] \quad (2.25)$$

At zero temperature,

$$j_{net}^s = \frac{Le}{h} \int_{\varepsilon_F}^{\varepsilon_F + eV} d\varepsilon_k T_s(\varepsilon_k) \quad (2.26)$$

$$j_{net}^s = \frac{Le}{h} eV T_s(\varepsilon_F) \quad (2.27)$$

$$j_{net}^s = \frac{Le^2}{h} T_s(\varepsilon_F) V. \quad (2.28)$$

When the electric field \mathbb{E} is not too big, one can approximate the current density to be proportional to the electric field as

$$j = \sigma \mathbb{E} \quad (2.29)$$

Because $j = \sigma \mathbb{E} = \sigma \frac{V}{d} = \frac{\sigma}{d} V$ and compare this equation with Eq. (2.29), one obtains

$$\frac{\sigma_s}{d} = \frac{Le^2}{h} T_s(\varepsilon_F) \quad (2.30)$$

$$\sigma_s = \frac{Le^2 d}{h} T_s(\varepsilon_F). \quad (2.31)$$

Once we obtain $T_s(\varepsilon_F)$ for each case, we can examine closely how each property of the middle layer affects the giant magnetoresistance.

CHAPTER III

MAGNETORESISTANCE RESULTS AND DISSCUSSION

In this chapter, we present the results of the magnetoresistance calculation for all three types of tri-layered systems: an insulating layer sandwiched by two ferromagnetic metals, a non-magnetic metal sandwiched by two ferromagnetic metals, and junctions with all three layers of ferromagnetic metals. We consider the following factors on the magnetoresistance in a small applied magnetic field for each type of junctions.

- 1) The thickness L of the middle layer.
- 2) The strength of the barrier potential of the insulating layer of FM/insulator/FM junction.
- 3) The quality of the interfaces between layers of FM/non-magnetic metal/FM and FM/FM/FM junctions.

In order to present the results in relatable numbers, for all of our results we take the ferromagnetic metal to be Fe and use its relevant physical quantities. That is, the Fermi energies $\varepsilon_{F1}, \varepsilon_{F3}$ of the ferromagnetic layers are taken to be the same and equal to $\varepsilon_F = 11$ eV. The molecular field energy h_0 is approximately 0.089 eV, which we approximate from the Curie temperature of Fe. The proportional constant related to the applied field C is taken to be the magnetic dipole moment of Fe which is equal to $2.22\mu_B = 0.13$ meV/T, where μ_B is the Bohr magneton.

3.1 Magnetoresistance of FM/insulator/FM systems

We first show the effect of the insulating layer thickness L on the magnetoresistance in a small applied field B in our model. We will make substitution of the related parameters in order to set the thickness to be in the range of 9 \AA to 18 \AA , which is consistent with most experiments. Also, because Al_2O_3 and MgO are used as the insulating layers in most experiments and their band gaps are between $7.0 \text{ eV} - 9.4 \text{ eV}$ (Lee et al., 2013; Chayed et al., 2011; Heo et al., 2015), we take our parameter U_0 , representing the insulating barrier height, to be in the range of 0.3 to 0.5 times of ε_F .

The plot of the magnetoresistances as a function of the magnetic field for the thicknesses of the insulating layer $L = 6/k_F$ and with $U_0 = 0.4\varepsilon_F$ is shown in Figure 3.1. Here, k_F is the magnitude of the Fermi wave vector of the itinerant electrons in the ferromagnetic layers. In our case we use Fe; therefore, $1/k_F \sim 2$ to 3 \AA .

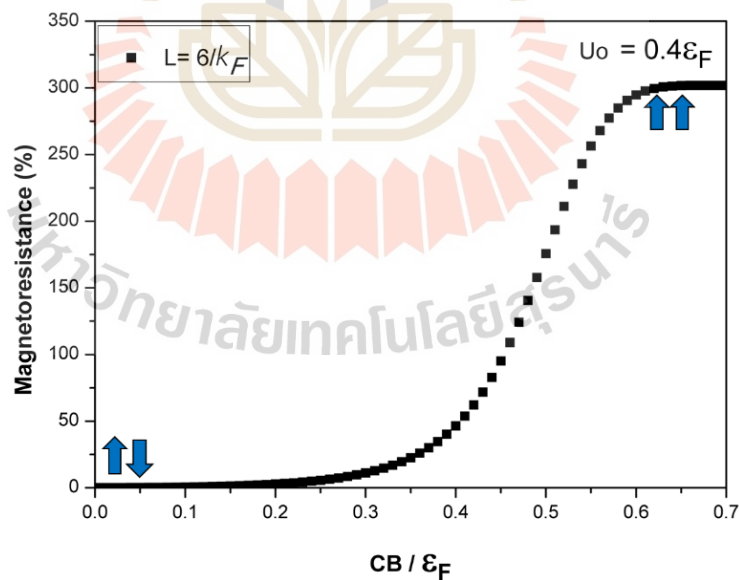


Figure 3.1 Magnetoresistance as a function of magnetic field with thickness of the insulating layer $L = 6/k_F$ and $U_0 = 0.4\varepsilon_F$.

In Figure 3.1, the magnetoresistance versus external magnetic field curve reveals that the magnetoresistance is increased at a small rate with small field. At some value, in this case CB around $0.4\varepsilon_F$, the rate of the increase becomes large and the magnetoresistance then reaches a maximum at a critical value of magnetic field (CB_C).

We show the effect of the change in thickness of insulating layer in Figure 3.2.

In Figure 3.2(a), we show a plot of the magnetoresistance as a function of external magnetic field for various thickness L ($L = 3/k_F, 4/k_F, 5/k_F, 6/k_F$) with $U_0 = 0.4\varepsilon_F$, and (b) we show experimental results of similar junctions. Although, qualitatively our theoretical model predicts the right trend of the dependence of the magnetoresistance on the thickness, quantitatively it predicts 10 times higher value.

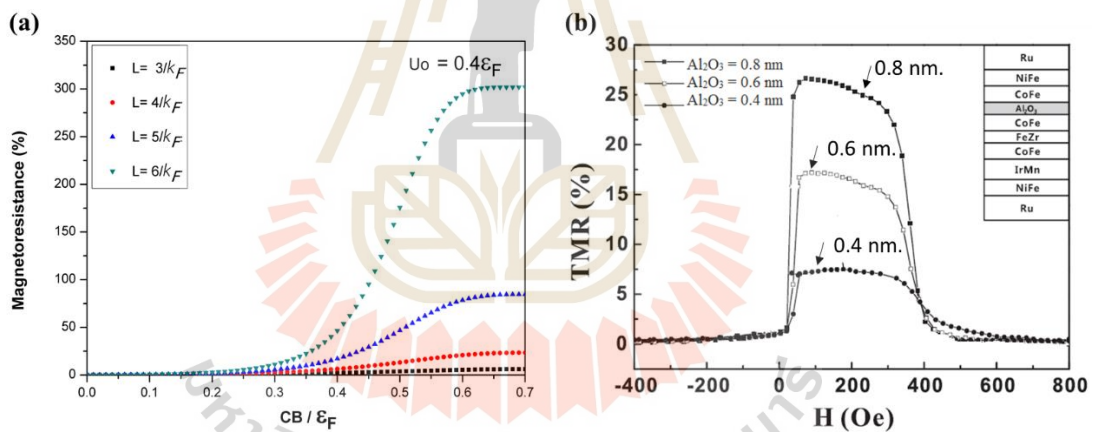


Figure 3.2 (a) Magnetoresistance as a function of magnetic field with varying thickness L of the insulating layer and $U_0 = 0.4\varepsilon_F$. (b) The Magnetoresistance of CoFe/ Al_2O_3 /CoFe with very thin tunnel barriers. The Al_2O_3 barrier was formed by oxidizing the Al_2O_3 thickness.

As mentioned in the literature part of experimental Al_2O_3 and MgO are used as the insulating layers. The energy band gap of Al_2O_3 and MgO equal to 7.4 and 7.8 eV

respectively. We take our parameter U_0 to be in the range of 0.33 with 0.35 times ε_F as shown in Figure 3.3.

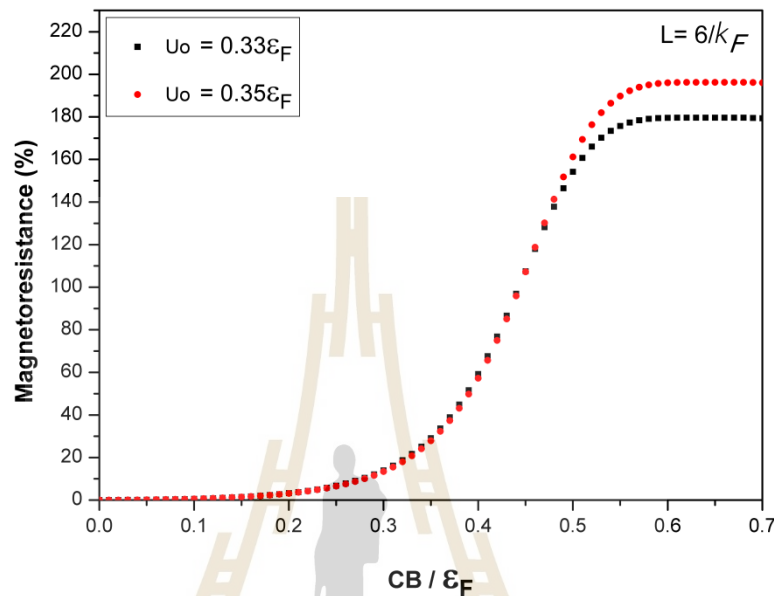


Figure 3.3 Magnetoresistance as a function of magnetic field with thickness $L = 6/k_F$ of the insulating layer when $U_0 = 0.33\varepsilon_F$ and $U_0 = 0.35\varepsilon_F$.

From Figure 3.3, the red dots represent the calculated magnetoresistance of the junction with MgO as insulating layer and the black ones do that of the junction with Al_2O_3 as insulating layer. Our simple model does predict that MgO would give higher magnetoresistance than Al_2O_3 would, which qualitatively agrees with experiments.

As mentioned earlier, the magnetoresistance is saturated, when the magnetic field is large enough. We call it a critical magnetic field (CB_c/ε_F). In Figure 3.4, we plot CB_c/ε_F as a function of insulating barrier height U_0/ε_F for $L = 6/k_F$. It is linear in U_0 . The plots of the magnetoresistance as (a) a function of L , when $U_0 = 0.40\varepsilon_F$ and $CB = 0.5\varepsilon_F$, and (b) the experiment work of tunneling magnetoresistance with thickness of Al_2O_3 are shown in Figure 3.3.

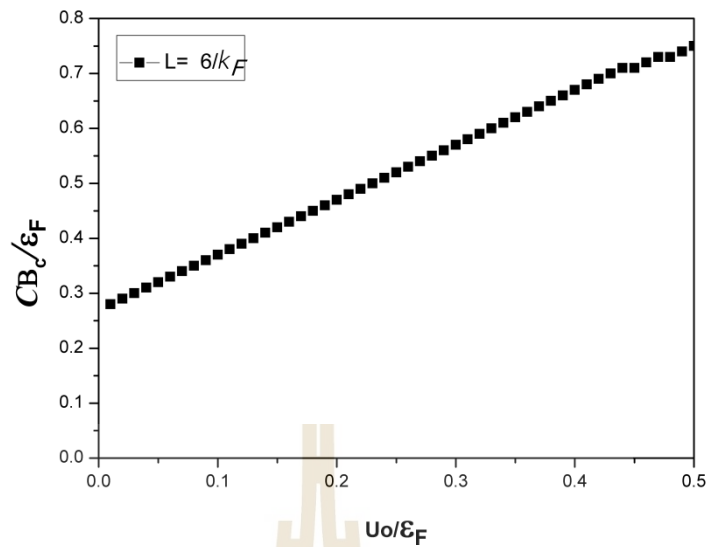


Figure 3.4 The critical magnetic field CB_c/ε_F versus potential barrier U_0/ε_F .

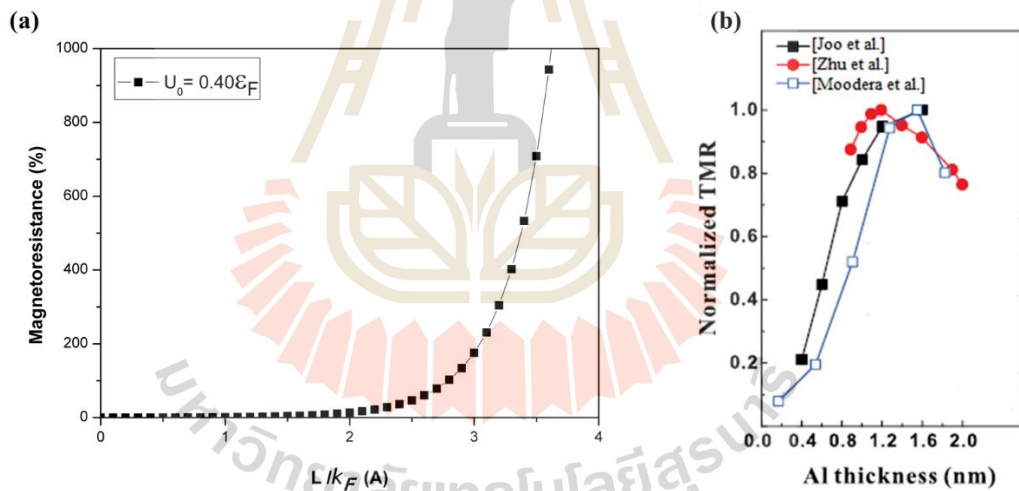


Figure 3.5 (a) graph magnetoresistance versus thickness when potential barrier $U_0 = 0.4\varepsilon_F$ our work. (b) the experiment work of tunneling magnetoresistance with thickness of Al_2O_3

Our model predicts that the magnetoresistance is qualitatively increased with the insulating-layer thickness. In reality, this increase stops at a particular thickness for each system. Our model cannot account for this fact, because it does not include the

interaction term known as Ruderman-Kittel-Kasuya-Yosidaand (RKKY) between the two ferromagnetic metals. This interaction depends on the thickness of the adjacent ferromagnetic layer.

3.2 Magnetoresistance of FM/non-magnetic metal/FM systems

Now, we show the effect of the non-magnetic metallic layer thickness L and the quality of the two FM/non-magnetic metal interfaces on the magnetoresistance in a small applied field B . As shown in Chapter II, we model the quality of the interfaces with a Delta-function barrier potential. We use a unitless parameter $Z \equiv \frac{mU}{h^2 k_F}$ to represent the potential. Small and large values of Z identify with metallic and tunneling contacts respectively. For our FM/non-magnetic metal/FM junctions, the parameters Z_1 and Z_2 represent the quality of contacts at the interface on the left and that on the right of the non-magnetic metallic layer respectively. Figure 3.6 contains the plots of magnetoresistance vs B when $\varepsilon_{F2}/\varepsilon_{F1} = 1.1$, mimicking Fe/Cr/Fe systems, and $Z_1 = Z_2 = 0.5$.

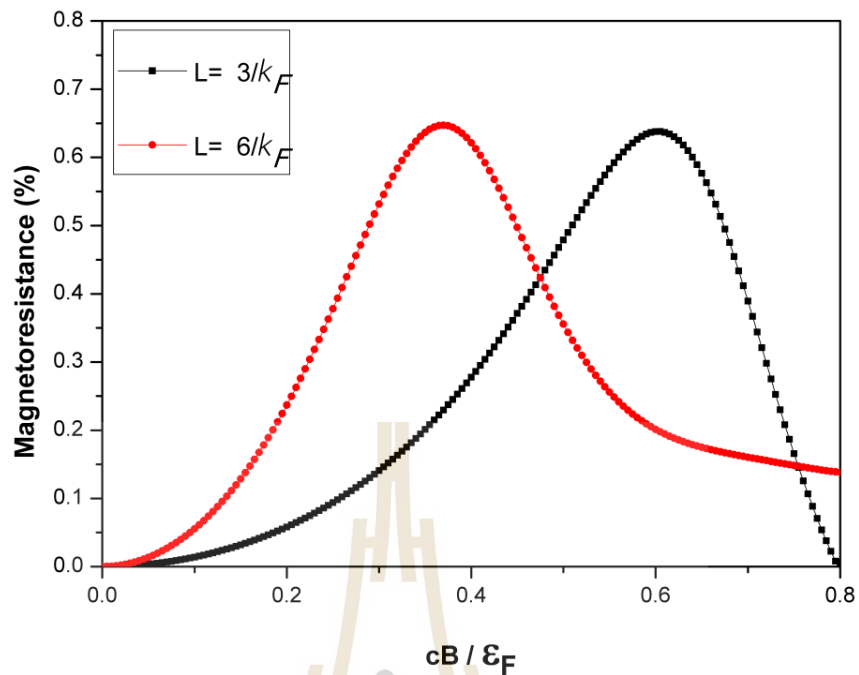


Figure 3.6 Magnetoresistance vs B at different values of L . $Z_1 = Z_2 = 0.5$ and $\varepsilon_{F2}/\varepsilon_{F1} = 1.1$.

As can be seen in Figure 3.6, the magnetoresistance is increased with the magnetic field and reaches a maximum and is then decreased with the field, unlike that in the case of FM/I/FM junction. Also, the maximum value of the magnetoresistance is insensitive to the thickness of the non-metallic layer. In Figure 3.7 we compare our results with those from Fert group. They are qualitatively similar.

When the thickness of the metallic layer changes, the magnetoresistance oscillates with the thickness as shown in Figure 3.8. In these plots, we take $CB = 0.7\varepsilon_F$. Figure 3.8(a) shows magnetoresistance vs the thickness for two values of $\varepsilon_{F2}/\varepsilon_{F1}$. The plots indicate that there is an optimum value of thickness that will result in a maximum value of magnetoresistance, which is consistent with Ruderman-Kittel-Kasuya-

Yosida and interaction. Figure 3.8(b) shows the experimental results. (Baibich et al., 1992).

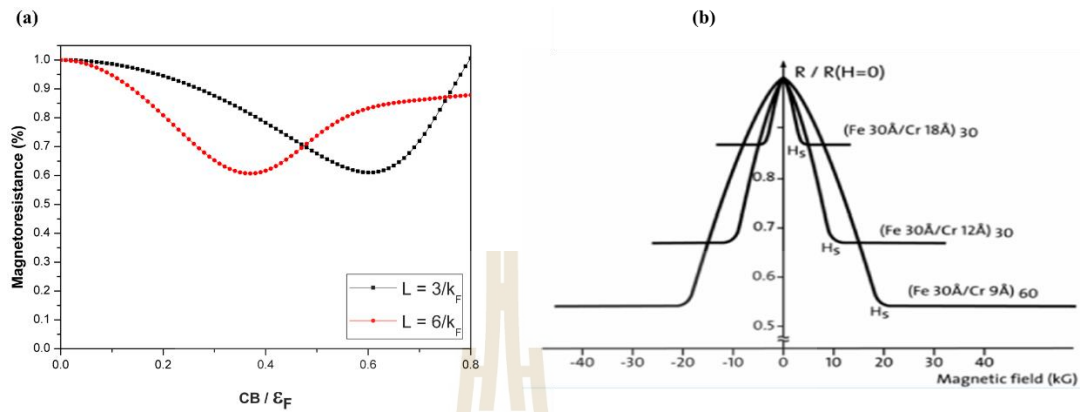


Figure 3.7 the graph shows MR vs CB/ϵ_F (a). Fert group used multilayers of the form $(Fe/Cr)_n$ resistance decreased at 4.2 K (b).

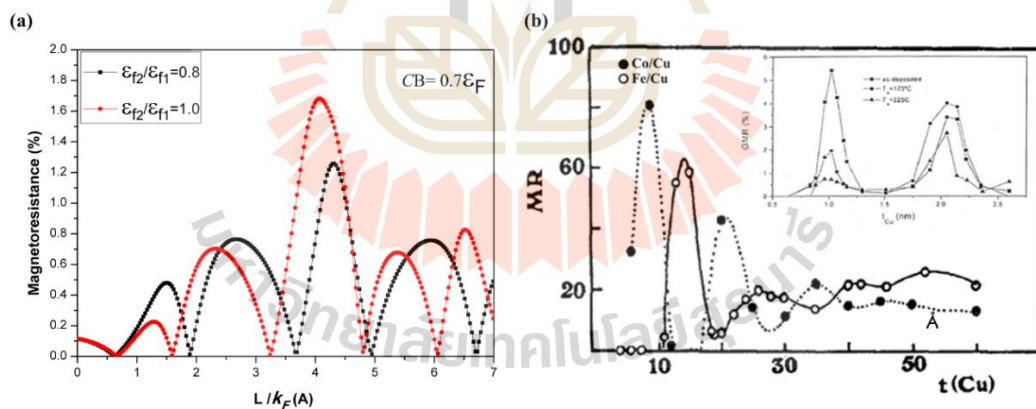


Figure 3.8 The graph shows MR vs thickness of middle layer (a). Variation of the magnetoresistance ratio of both $Fe(15 \text{ \AA})/Cu(t_{Cu})$ (open symbols) and $Co(15 \text{ \AA})/Cu(t_{Cu})$ (full symbols) superlattices as a function of the Cu layer thickness (b) (Baibich et al., 1992).

We can consider changing the metallic layer by varying the value of $\epsilon_{F2}/\epsilon_{F1}$. As we can see in Figure 3.9, changing the ratio results in the change in the maximum

value of the magnetoresistance. It suggests that if we want to obtain a big value for the magnetoresistance from FM/nonmagnetic metal/FM system, we should use a nonmagnetic metal that has similar value of the Fermi energy to that of the ferromagnetic layer.

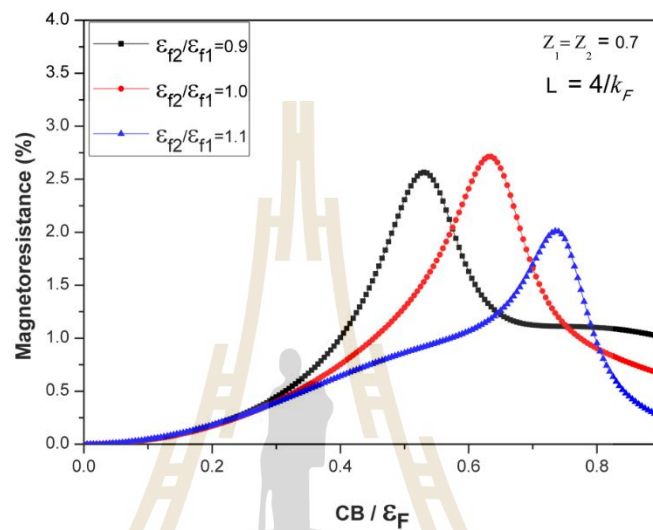


Figure 3.9 shows the variation of magnetoresistance (MR) values with external magnetic fields (CB) which change $\varepsilon_{F2}/\varepsilon_{F1}$ equal to 0.9 to 1.1 respectively. $Z_1 = Z_2 = 0.7$.

3.3 Magnetoresistance of FM/FM/FM systems

The magnetoresistance at various value of the thickness of the middle ferromagnetic layer are plotted in Figure 3.10 for $Z_1 = Z_2 = 1$. The maximum of magnetoresistance varies very much with the thickness and it happens at different values of the field; the thicker the higher.

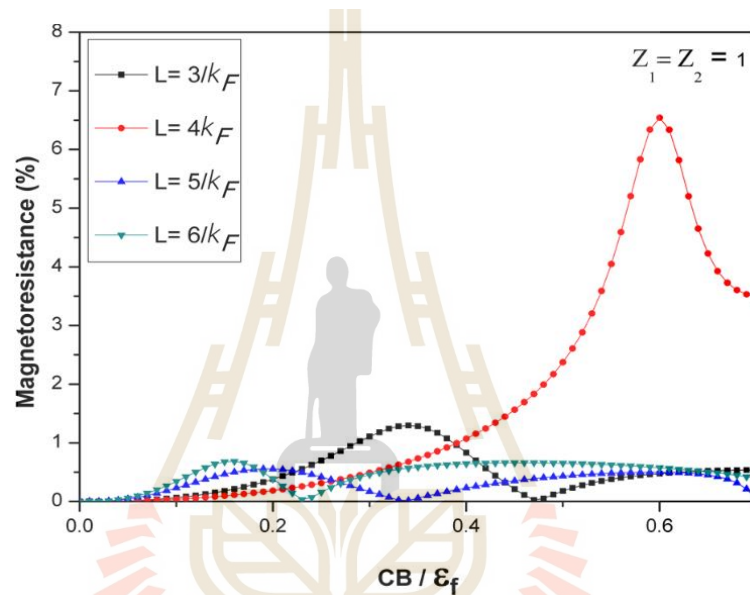


Figure 3.10 Magnetoresistance vs applied magnetic field at different values of L . $Z_1 = Z_2 = 1$ and $\varepsilon_{F2}/\varepsilon_{F1} = 1$.

Changing the thickness of the middle layer affects the magnetoresistance changes as seen in the plots in Figure 3.11. In these plots, we take $CB = 0.5\varepsilon_F$. These indicate that there is an optimum value of thickness L that will result in a maximum value of magnetoresistance, which is qualitatively consistent with result of FM/insulator/FM systems in Figure 3.7.

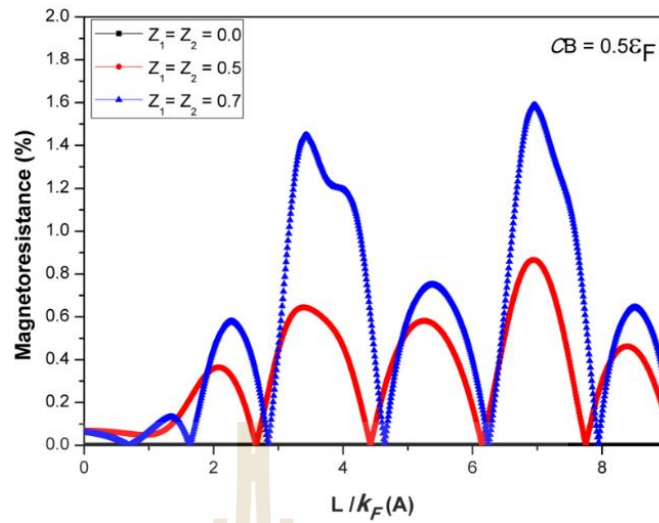


Figure 3.11 Represents the change of value magnetoresistance vs thickness L at various values of the parameter $Z = 0, 0.5, 0.7$. When constant $CB = 0.5\varepsilon_F$.

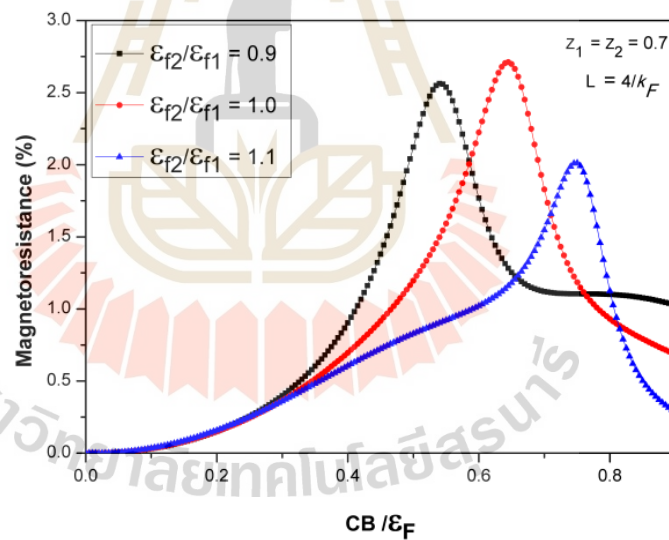


Figure 3.12 represents the change of value magnetoresistance vs thickness L at various values of the parameter $Z = 0, 0.5, 0.7$. $CB = 0.5\varepsilon_F$ for these plots.

We can consider changing the ferromagnetic metallic layer by varying the value of $\varepsilon_{F2}/\varepsilon_{F1}$ as shown in Figure 3.3.3. The results are quite similar to those in the

previous section. High magnetoresistance would be achieved when the ferromagnetic metals are similar.

Lastly the results in Figure 3.13 are the plots of the magnetoresistance as a function of CB for different qualities of the two junctions: $Z_1 = Z_2$ in Figure 3.13(a) and $Z_1 \neq Z_2$ in Figure 3.3.4(b). We take $L = 4/k_F$.

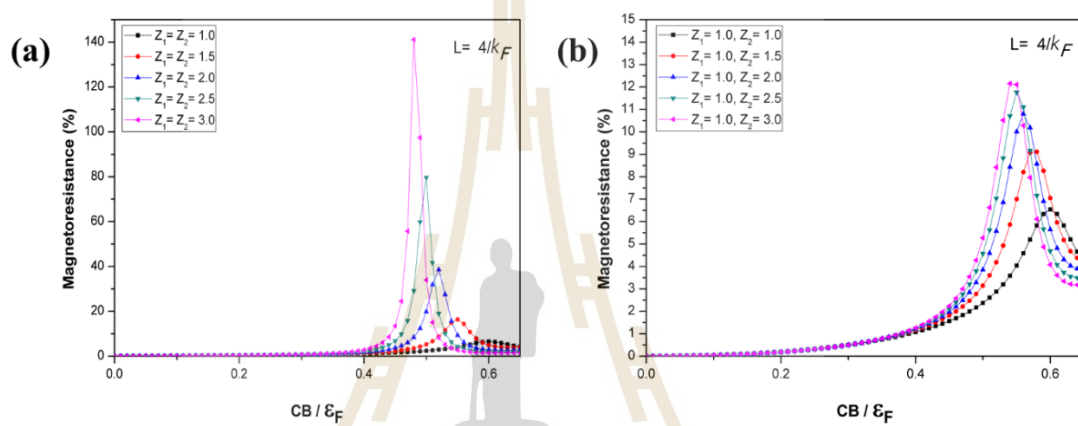


Figure 3.13 Show the result of magnetoresistance in a function of external magnetic field (CB/ϵ_F) of (a) $Z_1 = Z_2$ and (b) $Z_1 \neq Z_2$.

We can see that the value of Z significantly affects the magnetoresistance. In general, the higher value for Z the higher the magnetoresistance as well.

CHAPTER IV

CONCLUSION

In this work, we investigate the magnetoresistance of three types of tri-layered systems: FM/insulator/FM, FM/non-magnetic metal/FM, and FM/FM/FM junctions based on quantum principles to calculate the theoretical values under small external magnetic field. We take into account many factors that may affect the magnetoresistance, such as the thickness L of the middle layer, strength of the barrier potential (In the FM/insulator/FM junction.), and the quality of the interfaces between layers.

First of all, we present the results of FM/insulator/FM junction. When we consider the effect of the thickness of the insulating layer, our model predicts that the magnetoresistance is increased with the thickness. Also, it suggests that certain values of the barrier potential, or the band gap of the insulating layer, give the high magnetoresistance at each thickness.

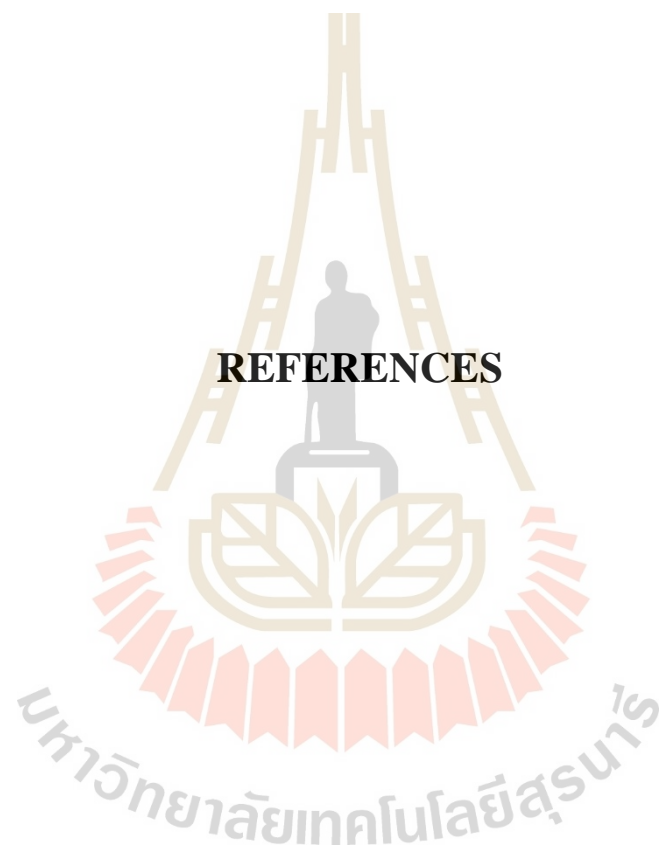
For the FM/non-magnetic metal/FM junction, the effect of the thickness of the non-magnetic metallic layer (L) is different from the previous case. That is, the increase in thickness does not increase the magnetoresistance. It shows oscillating behavior. In we work show that the quality of the two FM/non-magnetic metal interfaces (Z) has a huge effect on magnetoresistance. The result from the junction also shows that the (Z) value has a significant effect on the resistance. In other words, the resistance value is

greater by the Z value. Also in our model, certain thicknesses give the maximum magnetoresistance, which is consistent with experiments.

In the last case, FM/FM/FM junctions have the result of magnetoresistance looks like a seam FM/non-magnetic metal/FM such as the effect of thickness and the strength of the barrier potential. We emphasize the effect of the delta functions Z_1 and Z_2 which is a very thin insulator between the Ferrero region on the value of magnetoresistance on the resistance value in case of $Z_1 = Z_2$ and $Z_1 \neq Z_2$: the greater the value of Z , the bigger the magnetoresistance.



REFERENCES



REFERENCES

- Almasi, H., Sun, C. L., Li, X., Newhouse-Illige, T., Bi, C., Price, K. C., Nahar, S., Grezes, C., Hu, Q., Amiri, P., Wang, K. L., Voyles, P. M., and Wang, W. G. (2017). Perpendicular magnetic tunnel junction with W seed and capping layers. **Journal of Applied Physics**. 121.
- Althammer, M., Singh, A. V., Keshavarz, S., Yurtisigi, M. K., Mishra, R., Borisevich, A. Y., LeClair, P., and Gupta, A. (2016). Investigation of the tunnel magnetoresistance in junctions with a strontium stannate barrier. **Journal of Applied Physics**. 120.
- Autes, G., Mathon, J., and Umerski A. (2011). Theory of ultrahigh magnetoresistance achieved by k-space filtering without a tunnel barrier. **Physical Review B**. 83.
- Bai, X. J., Du, J., Zhang, J., You, B., Sun, L., Zhang, W., Wu, X. S., Tang, S. L., Hu, A., Hu, H. N., and Zhou, S. M. (2008). Giant magnetoresistance and tunnel magnetoresistance effects in FeCoGd-based spin valves and magnetic tunnel junctions. **Applied Physics Letters**. 103.
- Bai, Z., Cai, Y., Shen, L., Yang, M., Ko, V., Han, G., and Feng, Y. (2012). Magnetic and transport properties of $Mn_{3-x}Ga/MgO/Mn_{3-x}Ga$ magnetic tunnel junctions: A first-principles study. **Applied Physics Letters**. 100.
- Bakonyi, I., Péter, L., Rolik, Z., Kiss-Szabó, K., Kupay, Z., Tóth, J., Kiss, L. F., and Pádár, L. F. (2014). Decomposition of the magnetoresistance of multilayers into ferromagnetic and superparamagnetic contributions. **Physical Review B**. 70.

- Bakonyi, I., Simon, E., Tóth, B. G., Péter, L., and Kiss, L. F. (2009). Giant Magneto resistance in electrodeposited Co-Cu/Cu multilayers: Origin of the absence of oscillatory behavior. **Physical Review B**. 79.
- Bardeen, J. (1961). Tunneling from a many-particle point of view. **Physical Review Letters**. 6.
- Barness, D., and Frydman, A. (2005). Zero field resistance dip in magnetic tunnel junctions employing a granular electrode. **Physical Review B**. 72.
- Barraud, C., Deranlot, C., Seneor, P., Mattana, R., Dlubak, B., Fusil, S., Bouzehouane, K., Deneuve, D., Petroff, F., and Fert, A. (2010). Magnetoresistance in magnetic tunnel junctions grown on flexible organic substrates. **Applied Physics Letters**. 96.
- Brey, L., Tejedor, C., and Fernández-Rossier, J. (1996). Tunnel magnetoresistance in GaMnAs: Going beyond Jullière formula. **Applied Physics Letters**. 85.
- Butler, W. H., Zhang, X. G., Schulthess, T. C., and Laren, J. M. (2001). Spin-dependent tunneling conductance of Fe/MgO/Fe sandwiches. **Physical Review B**. 63.
- Castaño, F. J., Morecroft, D., and Ross, C. A. (2006). Low-field giant magnetoresistance in layered magnetic rings. **Physical Review B**. 74.
- Chayed, N. F., Badar, N., Rusdi, R., Kamarudin, N., and Kamarulzaman, N. (2011). Optical Band Gap Energies of Magnesium Oxide (MgO) Thin Film and Spherical Nanostructures. **AIP Conference Proceedings**. 1400.
- Chen, S. P., and Chang, C. R. (2009). Attenuated Oscillation of the Tunneling Magnetoresistance in a Ferromagnet-Metal-Insulator-Ferromagnet Tunneling Junction. **IEEE Transactions on Magnetics**. 45.

- Chiba, D., Sato, Y., Kita, T., and Ohno, H. (2004). Current-Driven Magnetization Reversal in a Ferromagnetic Semiconductor (Ga,Mn)As/GaAs/(Ga,Mn) As Tunnel Junction. **Physical Review Letters**. 93.
- Chowdhury, P., Ghosh, S. K., Dogra, A., Dey, G. K., Gowda, Y. G., Gupta, S. K., Ravikumar, G., Grover, A. K., and Suri, A. K. (2008). Structural evolution and giant magnetoresistance in electrodeposited Co-Cu/Cu multilayers. **Physical Review B**. 77.
- Christian, H., and Stiles, M. D. (2008). Ab initio studies of the spin-transfer torque in magnetic tunnel junctions. **Physical Review Letters**. 100.
- Chun, Y. Y., and Bader, S. D. (2002). Voltage controlled spintronic devices for logic applications. **Applied Physics**. 87.
- Diao, Z., Nowak, E. R., Haughey, K. M., and Coey, J. M. D. (2011). Nanoscale dissipation and magnetoresistive 1/f noise in spin valves. **Physical Review B**. 84.
- Dieny, B., and Chshiev, M. (2017). Perpendicular magnetic anisotropy at transition metal/oxide interfaces and applications. **Review of Modern Physics**. 89.
- Faure-Vincent, J., Tiusan, C., Jouguelet, E., Canet, F., and Sajieddine, M. (2003). High tunnel magnetoresistance in epitaxial Fe/MgO/Fe tunnel junctions. **Applied Physics Letters**. 82.
- Feng, Z., Yong, G., and Bing, L. G. (2002). Giant magnetoresistance effect in a magnetic-electric barrier structure. **Physical Review B**. 66.
- Fert, A. (2008). Nobel Lecture: Origin, development, and future of spintronics. **Review of Modern Physics**. 80.

- Fert, A., Wohlfarth, E. P., North, H., and Campbell, I. A. (1988). Transport properties of ferromagnets in ferromagnetic Materials. **Applied Physics Letters**. 61.
- García-García, A., Pardo, J. A., Štrichovanec, P., Magén, C., Vovk, A., Štrichovanec, P., Algarabel, P., Magén, C., De Teresa, J. M., Morellón, L., and Ibarra, M. R. (2010). Tunneling magnetoresistance in Fe/MgO granular multilayers. **Journal of Applied Physics**. 107.
- García-García, A., Pardo, J. A., Štrichovanec, P., Magén, C., and Vovk, A. (2011). Tunneling magnetoresistance in epitaxial discontinuous Fe/MgO multilayers. **Applied Physics Letters**. 78.
- Grünberg, P., Binasch, G., Saurenbach, F., and Zinn W. (1989). Enhanced magnetoresistance in layered magnetic structures with antiferromagnetic interlayer exchange. **Physical Review B**. 39.
- Guth, M., Dinia, A., Schmerber, G., and Berg, H. A. M. van den. (2001). Tunnel magnetoresistance in magnetic tunnel junctions with a ZnS barrier. **Applied Physics Letters**. 78.
- Hashimoto, T., Kamikawa, S., Soriano, D., Pedersen, J. G., Roche, S., and Haruyama, J. (2014). Tunneling magnetoresistance phenomenon utilizing graphene magnet electrode. **Applied Physics Letters**. 105.
- Hatanaka, S., Miwa, S., Matsuda, K., Nawaoka, K., Tanaka, K., Morishita, H., Goto, M., Mizuochi, N., Shinjo, T., and Suzuki, Y. (2015). Tunnel anisotropic magnetoresistance in CoFeB|MgO|Ta junctions. **Applied Physics Letters**. 107.
- Heo, S., Cho, E., Lee, H. I., Park, G. S., Kang, H. J., Nagatomi, T., Choi, P., and Choi, B. D. (2015). Band gap and defect states of MgO thin films investigated using reflection electron energy loss spectroscopy. **AIP Advances**. 5.

- Horst, H. (1978). Magnetic properties of thin ferromagnetic films in relation to their structure. **Thin Solid Films**. 223.
- Ikeda, S., Miura, K., Yamamoto, H., Mizunuma, K., Gan, H. D., Endo, M., Kanai, S., Hayakawa, J., Matsukura, F., and Ohno, H. (2010). A perpendicular-anisotropy CoFeB–MgO magnetic tunnel junction. **Nature Materials**. 9.
- Jiang, J. S., Pearson, J. E., and Bader, S. D. (2008). Absence of spin transport in the organic semiconductor Alq₃. **Physical Review B**. 77
- Joo, Sungjung., Jung, K. Y., Jun, K. I., Kim, D. S., Shin, K. H., Hong, J. K., Lee, B. C., and Rhie, K. (2014). Spin-filtering effect of thin Al₂O₃ barrier on tunneling magnetoresistance. **Applied Physics Letters**. 104.
- Julliere, M. (1975). Tunneling between ferromagnetic films. **Physics Letters A**. 54.
- Kasuya, T. (1954). The relaxation process in ferromagnetic resonance absorption. **Letters to the editor**. 803.
- Lee, K. A., Min, B. K., Byeon, Y. S., Choi, J. H., Jung, R. J., Uhm, H. S, and Choi, E. H. (2009). Measurement of Energy Band Structure of MgO, MgSrO and MgCaO Thin Film by their Secondary Electron Emission Coefficient due to Auger Neutralization. **Journal of Physics: Conference Series**. 417.
- Liang, S. H., Tao, L. L., Liu, D. P., Lu, Y., and Han, X. F. (2014). Spin dependent transport properties of Mn-Ga/MgO/Mn-Ga magnetic tunnel junctions with metal (Mg, Co, Cr) insertion layer. **Journal of Applied Physics**. 115.
- Liu, L., Zhan, Q., Yang, H., Li, H., Zhang, S., Liu, Y., Wang, B., Tan, X., and Li, R.W. (2016). Magnetostrictive GMR spin valves with composite FeGa/FeCo free layers. **AIP Advances**. 6.

- Mathon, J., and Umerski, A. (2001). Theory of tunneling magnetoresistance of an epitaxial Fe/MgO/Fe(001) junction. **Physical Review B**. 63.
- Matsumoto, R., Fukushima, A., Yakushiji, K., Yakata, S., Nagahama, T., Kubota, H., Katayama, T., Suzuki, Y., Ando, K., Yuasa, S., Georges, B., Cros, V., Grollier, J., and Fert, A. (2009). Spin-torque-induced switching and precession in fully epitaxial Fe/MgO/Fe magnetic tunnel junctions. **Physical Review B**. 80.
- Matsuura, Y. (2016). Tunneling magnetoresistance of silicon chains. **Journal of Applied Physics**. 119.
- Mavropoulos, P., Ležaić, M., and Blügel, S. (2005). Half-metallic ferromagnets for magnetic tunnel junctions by ab initio calculations. **Physical Review B**. 72.
- Meinert, M., Buker, B., Graulich, D., and Dunz, M. (2015). Large exchange bias in polycrystalline MnN/CoFe bilayers at room temperature. **Physical Review B**. 92.
- Mellergard, A., and McGreevy, R. L. (1997). Structural and magnetic disorder in GMR materials. **Physical Review B**. 234.
- Mitra, A., Barick, B., Mohapatra, J., Sharma, H., Meena, S. S., and Aslam, M. (2016). Large tunneling magnetoresistance in octahedral Fe₃O₄ nanoparticles. **AIP Advances**. 6.
- Miyazaki, T., and Tezuka, N. (1995). Giant magnetic tunneling effect in Fe/Al₂O₃/Fe junction. **Journal of Magnetism and Magnetic Materials**. 139.
- Moges, K., Honda, Y., Liu, H. X., Uemura, T., and Yamamoto, M. (2016). Enhanced half-metallicity of off-stoichiometric quaternary Heusler alloy Co₂(Mn,Fe)Si investigated through saturation magnetization and tunneling magnetoresistance. **Physical Review B**. 93.

- Mohammed, F. M., Ghaleb, A. H. M., Majeed, M. A., Mohammed, M. N., and Mohammed, N. S. (2015). Electronic configuration of Iron (Fe). **Advances in Applied Science Research**. 6.
- Moodera, J. S., Janusz, N., and Rene, J. M. (1998). Interface magnetism and spin wave scattering in ferromagnet-insulator-ferromagnet tunnel junctions. **Physical Review B**. 80.
- Moodera, J. S., Gallagher, E. F., Robinson, K., and Nowak, J. (1997). Optimum tunnel barrier in ferromagnetic-insulator-ferromagnetic tunneling structures. **Applied Physics Letters**. 70.
- Moodera, J. S., Kinder, L. R., Wong, T. M., and Meservey, R. (1995). Large magneto resistance at room temperature in ferromagnetic thin film tunnel junctions. **Physical Review Letters**. 74.
- Nobori, M., Nakano, T., Hasegawa, J., and Oomi, G. (2011). Pressure-induced half metallic gap transformation in Co_2MnSi observed by tunneling conductance spectroscopy. **Physical Review B**. 83.
- Okamura, S., Miyazaki, A., Sugimoto, S., Tezuka, N., and Inomata, K. (2005). Large tunnel magnetoresistance at room temperature with a full-Heusler alloy electrode. **Applied Physics Letters**. 86.
- O'Keeffe, A. P., Kasyutich, O. I., Schwarzacher, W., Oliveira, L. S., and Pasa, A. A. (1998). Giant magnetoresistance in multilayers electrodeposited on n- Si. **Applied Physics Letters**. 73.
- Parkin, S. S. P., Kaiser, C., Panchula, A., Philip M. R., Hughes, B., Samant, M., and Yang, S.H. (2004). Giant tunnelling magnetoresistance at room temperature with MgO (100) tunnel barriers. **Nature Mater**. 3.

- Peter, L., Weihnacht, V., Toth, J., Oogany, L., Schneider, C. M., and Bakonyi, I. (2006). Influence of superparamagnetic regions on the giant magnetoresistance of electrodeposited Co-Cu/Cu multilayers. **Journal of Magnetism and Magnetic Materials**.132.
- Pong, Philip W. T., and Egelhoff, William F. (2009). Enhancement of tunneling magnetoresistance by optimization of capping layer thicknesses in CoFeB/MgO/CoFeB magnetic tunnel junctions. **Applied Physics Letters**. 105.
- Qi, Y., Xing, D. Y., and Dong, J. (1998). Relation between Julliere and Slonczewski models of tunneling magnetoresistance. **Physical Review B**. 58.
- Rajasekaran, N., and Mohan, S. (2012). Giant Magnetoresistance in Electrodeposited Films: Current Status and the Influence of Parameters. **Taylor & Francis**.
- Ruderman, M. A., and Kittel, C. (1954). Indirect Exchange Coupling of Nuclear Magnetic Moments by Conduction Electrons. **Physical Review B**. 96.
- Saffarzadeh, A. (2008). Tunnel magnetoresistance of a single-molecule junction. **Journal of Applied Physics**. 104.
- Sankaran, K., Swerts, J., Couet, S., Stokbro, K., and Pourtois, G. (2016). Oscillatory behavior of the tunnel magnetoresistance due to thickness variations in Ta|CoFe|MgO magnetic tunnel junctions: A first-principles study. **Physical Review B**. 94.
- Shiomi, Y., and Saitoh, V. (2017). Linear magnetoresistance in a topological insulator Ru_2Sn_3 . **AIP Advances**. 7.
- Shvets, I. V., Grigorenko, A. N., and Mapps, D. J. (2005). Spin-polarized electron tunneling across magnetic dielectric. **Applied Physics Letters**. 86.

- Singh, M. P., Carvello, B., and Ranno, L. (2006). Giant magnetoresistance in an all oxide spacerless junction. **Applied Physics Letters**. 89.
- Slonczewski, J. C. (1989). Conductance and exchange coupling of two ferromagnets separated by a tunneling barrier. **Physical Review B**. 39.
- Steiner, R., and Ziemann, P. (2006). Magnetic switching of the superconducting transition temperature in layered ferromagnetic/ superconducting hybrids: Spin switch versus stray field effects. **Physical Review B**. 74.
- Tao, L., Liang, S. H., Liu, D. P., Wei, H. X., Wang, J., and Han, X. F. (2014). Tunneling magnetoresistance in $\text{Fe}_3\text{Si}/\text{MgO}/\text{Fe}_3\text{Si}(001)$ magnetic tunnel junctions. **Applied Physics Letters**. 104.
- Tóth, B. G., Péter, L., Pogány, L., and Bakonyia, I. (2014). Preparation, Structure and Giant Magnetoresistance of Electrodeposited Fe-Co/Cu Multilayers. **Journal of The Electrochemical Society**. 161.
- Tripathy, D., and Adeyeye, A. O. (2007A). Effect of spacer layer thickness on the magnetic and magnetotransport properties of $\text{Fe}_3\text{O}_4/\text{Cu}/\text{Ni}_{80}\text{Fe}_{20}$ spin valve structures. **Physical Review B**. 75.
- Tripathy, D., and Adeyeye, A. O. (2007B). Magnetic and tunneling magnetoresistive properties of an all-oxide $\text{Fe}_3\text{O}_4\text{-Al}_2\text{O}_3$ granular system. **Physical Review B**. 76.
- Tsunegi, S., Sakuraba, Y., Oogane, M., Naganuma, H., Takanashi, K., and Ando, Y. (2009). Enhancement in tunnel magnetoresistance effect by inserting CoFeB to the tunneling barrier interface in $\text{Co}_2\text{MnSi}/\text{MgO}/\text{CoFe}$ magnetic tunnel junctions. **Applied Physics Letters**. 94.
- Tsymbal, E. Y., Burlakov, V. M., and Oleinik, I. I. (2002). Spin injection into amorphous semiconductors. **Physical Review B**. 66.

- Tsymbal, E. Y., and Pettifor, D. G. (1996). Effects of band structure and spin independent disorder on conductivity and giant magnetoresistance in Co/Cu and Fe/Cr multilayers. **Physical Review B**.39.
- Tsymbal, E. Y., Sokolov, A., Sabirianov, I. F., and Doudin, B. (2003). Resonant inversion of tunneling magnetoresistance. **Physical Review Letters**. 90.
- Wang, L., Wang, S. G., Syed Rizwan, Q. H., and Han, X. F. (2009). Magnetoresistance effect in antiferromagnet/nonmagnet/antiferromagnet multilayers. **Applied Physics Letters**. 95.
- Wang, T., Yang, Z., Wang, W., Si, M., Yang, D., Liu, H., and Xue, D. (2017). Large magnetoresistance effect in nitrogen-doped silicon. **AIP Advances**. 7.
- Wong, P. K., Evetts, J. E., Yang, Z., and Blamire, M. G. (1998). High conductance Magnetoresistive tunnel junctions with multiply oxidized barrier. **Journal of Applied Physics**. 83.
- Wu, H. C., Mryasov, O. N., Radican, K., and Shvets, I. V. (2009). Tunneling interlayer exchange coupling between oxide ferrimagnets: Analysis for Fe₃O₄ / vac / Fe₃O₄ case. **Applied Physics Letters**. 94.
- Yang, H. X., Chshiev, M., Kalitsov, A., Schuhl, A., and Butler, W. H. (2010).Effect of structural relaxation and oxidation conditions on interlayer exchange coupling in Fe | MgO | Fe tunnel junctions. **Applied Physics Letters**. 96.
- Yosida, K. (1957). Magnetic Properties of Cu-Mn Alloys. **Physical Review B**. 106.
- You, C. Y., Tian, N., Goripati, H. S., and Furubayashi, T. (2010). Current perpendicular-to-the-plane giant magnetoresistance of an all-metal spin valve structure with magnetic layer. **Applied Physics Letters**. 96.

- Yu, J. H., Lee, H. M., Ando, Y., and Miyazaki, T. (2003). Electron transport properties in magnetic tunnel junctions with epitaxial NiFe (111) ferromagnetic bottom electrodes. **Applied Physics Letters**. 82.
- Yuasa, S. (2002). Spin-Polarized Resonant Tunneling in Magnetic Tunnel Junctions. **American Association for the Advancement of Science**. 297.
- Yuasa, S., Nagahama, T., Fukushima, A., Suzuki, Y., and Ando, K. (2004). Giant roomtemperature magnetoresistance in single-crystal Fe/MgO/Fe magnetic tunneljunctions. **Nature Mater**. 3.
- Zhang, D. L., Song, X. H., Zhang, X., and Zhang, X.-G. (2014). Magnetoresistance of Au films. **Applied Physics Letters**. 116.
- Zhang, W. S., and Li, B. (1996). Spin-polarized tunneling and magnetoresistance in ferromagnet/insulator(semiconductor) single and double tunnel junctions subjected to an electric field. **Physical Review B**. 56.
- Zhang, W. S., Li, B. Z., and Zhang, X. (1998). Conductance magnetoresistance and interlayer coupling in tunnel junctions modulated by nonmagnetic metallic interlayers. **Applied Physics Letters**. 83.
- Zhu, W., Hirschmugl, C. J., Laine, A. D., Sinkovic, B., and Parkin, S. S. P. (2001). Determination of the thickness of Al oxide films used as barriers in magnetic tunneling junctions. **Applied Physics Letters**. 78.

CURRICULUM VITAE

Name: Mr. Adithep Butburee

Date of birth: 3 July 1990

Place of birth: Nakhon Phanom, Thailand

Nationality: Thai

Education

Academic year

2009-2012 Khon Kaen University, Khonkean, Khon Kaen, Thailand.

Bachelor of Science (Physics)

2013-2018 Suranaree University of Technology, Nakhon Ratchasima, Thailand.

Master of Science (Applied Physics)